

Directed Assembly of Metal–Cyanide Cluster Magnets

LIANNE M. C. BELTRAN AND
JEFFREY R. LONG*

Department of Chemistry, University of California,
Berkeley, California 94720

Received July 13, 2004

ABSTRACT

The simple, well-understood coordination chemistry of the cyanide ligand is of significant utility in the design of new single-molecule magnets. Its preference for bridging two transition metals in a linear $M'-CN-M$ geometry permits the use of multidentate blocking ligands in directing the assembly of specific molecular architectures. This approach has been employed in the synthesis of numerous high-nuclearity constructs, including simple cubic $M_4M'_4(CN)_{12}$ and face-centered cubic $M_8M'_6(CN)_{24}$ coordination clusters, as well as some unexpected cluster geometries featuring as many as 27 metal centers. The ability to substitute a range of different transition metal ions into these structures enables adjustment of their magnetic properties, facilitating creation of high-spin ground states with axial magnetic anisotropy. To date, at least four different cyano-bridged single-molecule magnets have been characterized, exhibiting spin-reversal barriers as high as 25 cm^{-1} . Ultimately, it is envisioned that this strategy might lead to molecules possessing much larger barriers with the potential for storing information at more practical temperatures.

Introduction

More than a decade ago, it was discovered that $[Mn_{12}O_{12}(O_2CCH_3)_{16}(H_2O)_4]$ exhibits magnetic bistability.¹ As depicted in Figure 1, this molecular cluster has a disc-shaped core consisting of a central $Mn^{IV}_4O_4$ cubane unit surrounded by a ring of eight oxo- and acetato-linked Mn^{III} centers. Antiferromagnetic coupling between the inner Mn^{IV} centers and the outer, high-spin Mn^{III} centers results in an $S = 10$ ground state. Remarkably, a negative axial zero-field splitting, D , leads to a loss in the degeneracy of the associated M_S sublevels, such that $M_S = +10$ and $M_S = -10$ are lowest in energy (see Figure 2). Thus, owing to the selection rule of $\Delta M_S = \pm 1$, there exists an energy barrier of $U = S^2|D|$ for conversion of “spin up” to “spin down” in the ground state. In this case, with $S = 10$ and $D = -0.5\text{ cm}^{-1}$, the magnitude of the spin-reversal barrier is approximately 50 cm^{-1} , leading to magnetic blocking at temperatures below 4 K, as evidenced by magnetic hysteresis loops.^{1b} Consequently, molecules possessing a

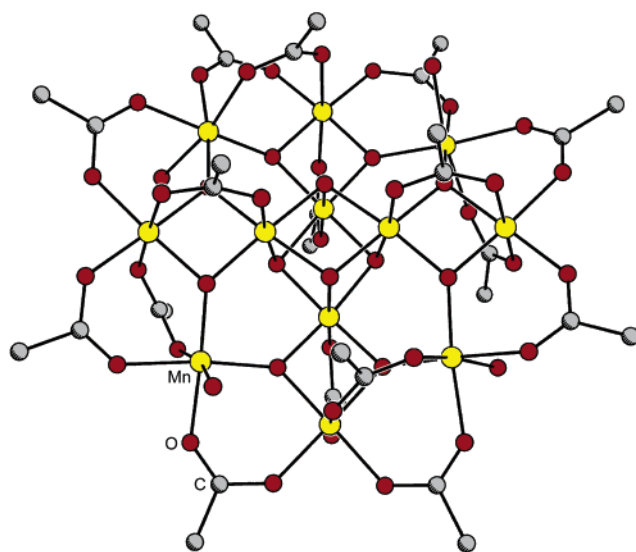


FIGURE 1. Disc-shaped cluster $[Mn_{12}O_{12}(O_2CCH_3)_{16}(H_2O)_4]$.

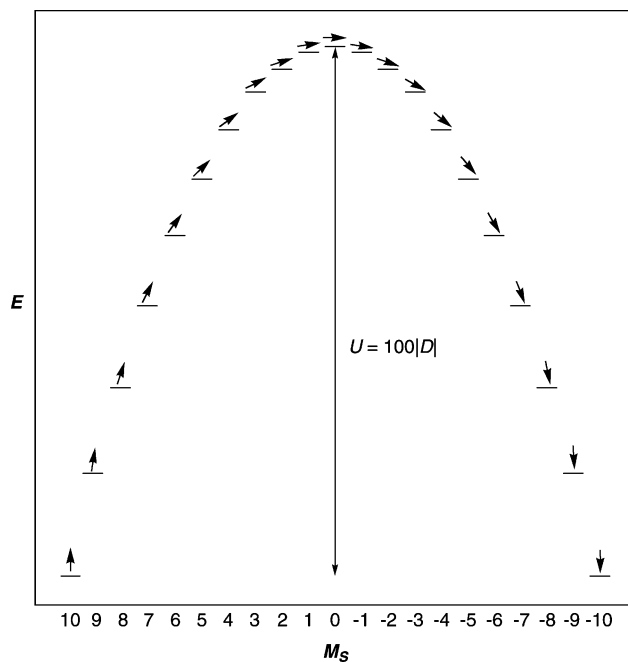


FIGURE 2. Energy level diagram for an $S = 10$ ground state with an axial zero-field splitting of $D < 0$, showing the spin-reversal barrier $U = S^2|D| = 100|D|$. The arrow above each M_S energy level represents the relative orientation of the spin with respect to the easy axis of the molecule. Note that, lacking an $M_S = 0$ level, a half-integral spin state would instead have a barrier of $U = (S^2 - 1/4)|D|$.

high-spin ground state with negative axial zero-field splitting are now commonly referred to as single-molecule magnets.

The magnet-like behavior of the Mn_{12} cluster has sparked the idea that information might one day be stored as the direction of the magnetization in individual molecules. With a diameter of roughly 1 nm for each bit, a close-packed array of molecules might achieve a surface density as high as 200 000 gigabits/in², representing an improvement of perhaps 3 orders of magnitude over

Lianne M. C. Beltran was born in Winnipeg, Canada, in 1979. She received a B.Sc. from the University of Western Ontario in 2001 and is currently a graduate student at the University of California, Berkeley. Her research focuses on the synthesis and characterization of inorganic clusters exhibiting unusual magnetic and photomagnetic properties.

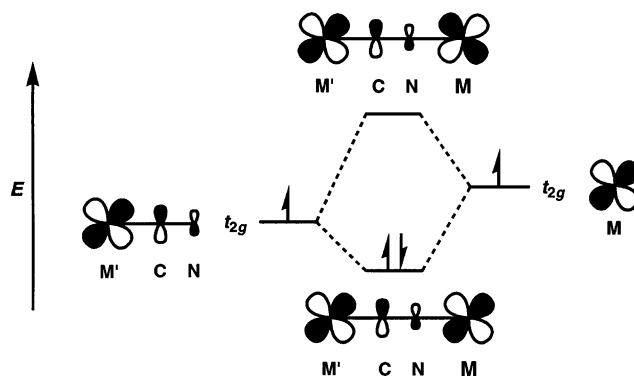
Jeffrey R. Long was born in Rolla, Missouri in 1969. He received a B.A. from Cornell University in 1991 and a Ph.D. from Harvard University in 1995. He has been on the faculty at the University of California, Berkeley, since 1997 and is currently an Associate Professor. His research involves the development of new synthetic methods for controlling the structures and properties of inorganic clusters and solids.

existing magnetic alloy film technologies. Such an improvement would be of particular importance for computer hard drives, where the distances between bits of information relates to the speed and efficiency of the drive. Obviously, there are formidable challenges to be overcome before a technology of this type could be implemented, not least of which is how to read and write data using such miniscule magnetic moments. One challenge, however, falls squarely within the domain of inorganic chemistry: Can we synthesize molecules with higher spin-reversal barriers, capable of storing information at more practical temperatures? It should be noted that there are numerous additional reasons for interest in these molecules, including exploration of the basic physics arising in the regime between molecular and bulk magnetism, as well as possible applications in quantum computing and magnetic refrigeration.²

More than 30 single-molecule magnets have been identified to date, by far the majority of which are transition metal-oxo clusters.² Despite recognition that metal ions such as Mn^{III} are particularly well-suited for generating the requisite magnetic anisotropy, progress in enhancing the spin-reversal barrier has been limited. Indeed, a variation on the original Mn₁₂ cluster still holds the record, with AC susceptibility measurements indicating an effective barrier of $U_{\text{eff}} = 56 \text{ cm}^{-1}$ for [Mn₁₂O₁₂(O₂-CCH₂Br)₁₆(H₂O)₄].³ The problem lies in our lack of ability to control the assembly of specific new transition metal-oxo structures, which arises from the fact that oxygen can bridge anywhere from two to six metal centers, with a wide flexibility in the M–O–M angles. Moreover, the pairwise magnetic exchange interactions within a cluster are highly sensitive to local geometry, making it almost impossible to predict the magnetic properties of a complex structure. As a result, the search for new metal-oxo single-molecule magnets remains a largely serendipitous process.

As an alternative bridging ligand, cyanide presents the possibility of overcoming certain of the aforementioned difficulties. Its preference for binding just two metal centers, one at each end, to afford a linear bridging arrangement is well-established. Consequently, solution assembly reactions can be devised with the expectation that the product will contain linear M'–CN–M moieties, providing some modicum of structural control. In addition, given this linear bridging arrangement, it is possible to predict the nature of the magnetic exchange coupling between octahedrally coordinated M' and M centers (see Figure 3).⁴ Unpaired spin density from metal-based orbitals of compatible symmetry ($t_{2g} + t_{2g}$ or $e_g + e_g$) will leak over into the same cyanide-based orbitals, leading to antiferromagnetic exchange via the Pauli exclusion principle. In contrast, the unpaired spin density from orthogonal metal-based orbitals ($t_{2g} + e_g$) will leak over into orthogonal cyanide-based orbitals, leading to ferromagnetic exchange via Hund's rules. The antiferromagnetic interaction is generally stronger and will tend to dominate the superexchange in a competitive situation. This predictive power should be of utility in the design of cyano-bridged molecules with high-spin ground states.

Antiferromagnetic Exchange Coupling:



Ferromagnetic Exchange Coupling:

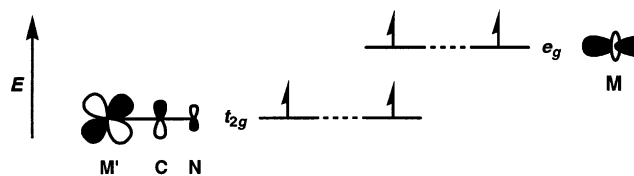
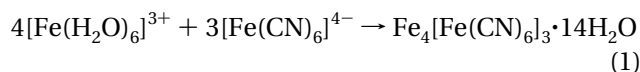
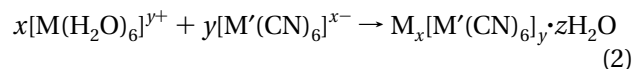


FIGURE 3. Orbital interaction diagrams for a M'–CN–M unit with octahedral coordination at the metal centers.

Without doubt, the most extensively studied metal–cyanide compound is the solid pigment Prussian blue. This compound is readily prepared by addition of ferric ions to an aqueous solution containing ferrocyanide:



Here, the nitrogen end of cyanide displaces water to form linear Fe^{II}–CN–Fe^{III} linkages, generating an extended structure based upon the three-dimensional framework depicted in Figure 4. The reaction can be extended to encompass a wide range of octahedral hexaquo and hexacyano complexes, leading to a large family of Prussian blue analogues, all adopting the same cubic structure type:



Note the essential difference between the two metal sites within the framework: M' is coordinated by the carbon end of six surrounding cyanide ligands and experiences a strong ligand field, while M is coordinated by the nitrogen end of six surrounding cyanide ligands and experiences a weaker ligand field. Since many different paramagnetic metal centers can be substituted onto these sites, the magnetic properties of the resulting solids are highly adjustable. Indeed, with the use of early transition metals in low oxidation states (i.e., metal ions with diffuse valence d orbitals having a large overlap with cyanide-based orbitals), chemists have produced Prussian blue analogues that exhibit bulk magnetic ordering at temperatures well above room temperature.⁵ This is exactly the type of substitutional control we hope to achieve, albeit in molecular clusters rather than extended solids.

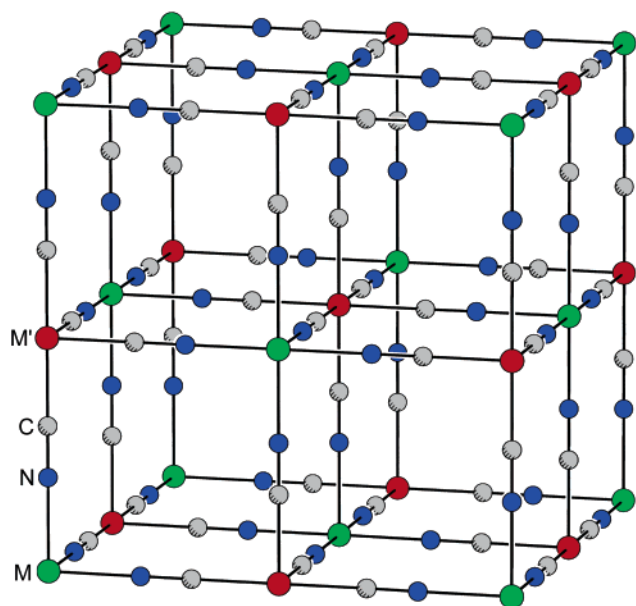
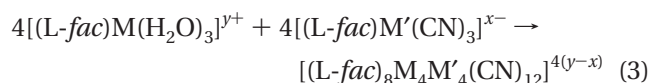


FIGURE 4. Unit cell for a Prussian blue type solid, $M[M'(CN)_6] \cdot zH_2O$, with no framework vacancies. Guest water molecules are omitted for clarity. In Prussian blue itself, $M' = Fe^{II}$, $M = Fe^{III}$, and one-quarter of the $[Fe(CN)_6]^{4-}$ units are missing from the lattice.

Herein, we present a straightforward approach to the synthesis of metal–cyanide coordination clusters, enabling the manipulation of ground-state spin and anisotropy as a means of attaining new single-molecule magnets. Although the focus will be on results originating from our laboratory, it is important to recognize that a number of other research groups have independently developed a similar approach.^{2,6}

Simple Cubic Clusters

As an initial test of our ability to direct the formation of specific metal–cyanide clusters, we set out to synthesize just one of the fundamental cubic cage units of the Prussian blue structure type as a discrete molecular entity. In an assembly process paralleling reaction 2, this requires use of blocking ligands capable of capping three *fac* positions in the octahedral coordination environment of each metal center. Taking advantage of the chelate effect, a tridentate ligand, *L-fac*, constrained so as to coordinate only in a *fac* mode, would be particularly well-suited for this purpose. With one such ligand on each precursor complex, a generic reaction through which a cubic cluster might assemble can be formulated:



The macrocyclic ligand 1,4,7-triazacyclononane (tacn) was selected for use as *L-fac* on recognition that steric hindrance would not prevent formation of a cube and that its 3-fold symmetry would eliminate the possibility of producing many different geometric isomers. In accord with reaction 3, $[(tacn)Co(H_2O)_3]^{3+}$ and $[(tacn)Co(CN)_3]^{3-}$ were found to react in boiling aqueous solution to afford

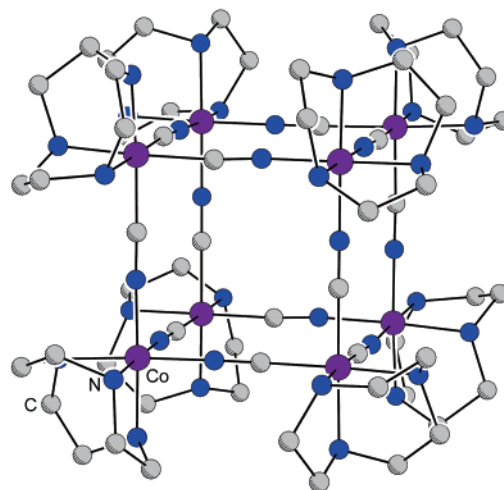


FIGURE 5. Cubic cluster $[(tacn)_8Co_8(CN)_{12}]^{12+}$.

Table 1. Variation of the Magnetic Properties for Established and Hypothetical Cubic $M_4M'_4(CN)_{12}$ Clusters

| M | M' | coupling ^a | S | example | ref |
|-------------------|-------------------|-----------------------|------------------|---|-----|
| Co ^{III} | Co ^{III} | N | 0 | $[(tacn)_8Co_8(CN)_{12}]^{12+}$ | 7 |
| Co ^{III} | Rh ^{III} | N | 0 | $[Cp^*_4Cp_4Co_4Rh_4(CN)_{12}]^{4+}$ | 9 |
| Mo ⁰ | Rh ^{III} | N | 0 | $\{[Cp^*_4(CO)_{12}Mo_4Rh_4(CN)_{12}] \supset K\}^{3-}$ | 10 |
| Cr ^{III} | Co ^{III} | N | $3/2 (\times 4)$ | $[(tacn)_8Cr_4Co_4(CN)_{12}]^{12+}$ | 7 |
| Co ^{II} | Co ^{III} | N | $3/2 (\times 4)$ | $[(tach)_4(H_2O)_{12}Co_8(CN)_{12}]^{8+}$ | 11 |
| Ni ^{II} | Co ^{III} | N | $1 (\times 4)$ | $[(tach)_4(H_2O)_{12}Ni_4Co_4(CN)_{12}]^{8+}$ | 11 |
| Cr ^{III} | Cr ^{III} | A | 0 | | |
| Cr ^{III} | V ^{III} | A | 2 | | |
| Mn ^{II} | Cr ^{III} | A | 4 | | |
| Ni ^{II} | Fe ^{III} | F | 6 | $[(tach)_4(H_2O)_{12}Ni_4Fe_4(CN)_{12}]^{8+}$ | 11 |
| Mn ^{II} | Fe ^{III} | A | 8 | | |
| Ni ^{II} | Cr ^{III} | F | 10 | | |

^a A = antiferromagnetic; F = ferromagnetic; N = no coupling.

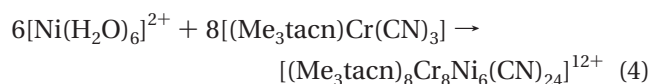
the cubic cluster $[(tacn)_8Co_8(CN)_{12}]^{12+}$.⁷ Figure 5 displays the structure of this product, which indeed consists of a single cage excised from the extended framework of a Prussian blue type solid.

A remarkable advantage of metal–cyanide chemistry is that once a stable new construct is identified, one can be reasonably confident that it will be possible to substitute certain other metal ions into the structure. Table 1 enumerates the different combinations of metal ions that have been incorporated into cubic $M_4M'_4(CN)_{12}$ clusters,^{7–11} together with some hypothetical combinations involving paramagnetic metal centers. Early on, Rauchfuss and co-workers established that cyclopentadienyl type ligands could be used as the *L-fac* capping groups in producing cubes via reaction 3.⁹ While their approach has not yet been employed in generating paramagnetic clusters, it is highly likely that it could be effective in doing so. The cluster $[(tacn)_8Cr_4Co_4(CN)_{12}]^{12+}$ features four paramagnetic Cr^{III} ($S = 3/2$) centers; however, these are located at alternating corners of the cube with diamagnetic Co^{III} centers situated at the intervening corners. Consequently, magnetic susceptibility measurements revealed no evidence of magnetic exchange coupling at temperatures down to 5 K.⁷ This is typical for cyano-bridged compounds: magnetic exchange coupling occurs between nearest neighboring spin centers but is extremely weak or negligible between next-nearest neighbors. Unexpected-

edly, it was found that the hydrogen bonding properties of 1,3,5-triaminocyclohexane (tach) enable it to stabilize cubic clusters with just water providing the terminal ligands at alternating cube vertices.¹¹ One of the resulting species, $[(\text{tach})_4(\text{H}_2\text{O})_{12}\text{Ni}_4\text{Fe}_4(\text{CN})_{12}]^{8+}$, is the only cube yet characterized in which the metals at both sites are paramagnetic. Here, magnetic susceptibility data indicates the presence of weak ferromagnetic exchange interactions with a coupling constant of $J = +5.5 \text{ cm}^{-1}$, giving rise to an $S = 6$ ground state. As discussed earlier, ferromagnetic coupling is precisely what is expected between low-spin Fe^{III} (t_{2g}^5) and Ni^{II} ($t_{2g}^6e_g^2$) centers connected through cyanide.⁴ The magnetic properties predicted similarly for other selected combinations of paramagnetic ions are given in Table 1. Note that the maximum spin ground state achievable for a cubic $\text{M}_4\text{M}'_4(\text{CN})_{12}$ cluster is $S = 10$, corresponding to ferromagnetic coupling between Cr^{III} (t_{2g}^3) and Ni^{II} ($t_{2g}^6e_g^2$) centers. This is the same as the spin of the ground state of $[\text{Mn}_{12}\text{O}_{12}(\text{O}_2\text{CCH}_3)_{16}(\text{H}_2\text{O})_4]$; if possible, we should like to do considerably better.

Face-Centered Cubic Clusters

To obtain significantly higher spin ground states, it is necessary to develop methods for constructing larger clusters, wherein more metal centers can be magnetically coupled. In assembly reaction 3, each precursor complex bears a blocking ligand, *L-fac*. Suppose a blocking ligand were present on only one of these reactants. This might allow growth of the metal–cyanide framework to continue further before the structure closes up into a cage. The reaction between $[\text{Ni}(\text{H}_2\text{O})_6]^{2+}$ and $[(\text{Me}_3\text{tacn})\text{Cr}(\text{CN})_3]$ ($\text{Me}_3\text{tacn} = N,N,N'$ -trimethyl-1,4,7-triazacyclononane) in boiling aqueous solution gives just such a result:⁸



As depicted in Figure 6, the 14-metal cluster product has a core structure wherein eight Cr^{III} ions are situated at the corners of a cube and are connected through cyanide bridges to six Ni^{II} ions, one located just above the center of each cube face. Note that each cyanide ligand is oriented such that its carbon end is bound to a Ni^{II} center, whereas in the precursor complex $[(\text{Me}_3\text{tacn})\text{Cr}(\text{CN})_3]$ the carbon atoms are bound to a Cr^{III} center. Apparently, the thermal energy delivered by heating the reaction is sufficient to induce isomerization of the cyanide ligand, yielding the thermodynamically favored $\text{Ni}^{\text{II}}\text{—CN—Cr}^{\text{III}}$ orientation. Unfortunately, when confronted with the strong-field carbon end of cyanide, the Ni^{II} centers convert to a square planar coordination geometry with a diamagnetic electron configuration. Thus, the cyanide isomerization destroys the desired ferromagnetic coupling between the Cr^{III} and Ni^{II} centers, and the magnetic properties of $[(\text{Me}_3\text{tacn})_8\text{Cr}_8\text{Ni}_6(\text{CN})_{24}](\text{NO}_3)_{12} \cdot 17\text{H}_2\text{O}$ are consistent with eight isolated Cr^{III} ($S = 3/2$) centers with the onset of only very weak antiferromagnetic coupling becoming apparent below 30 K.

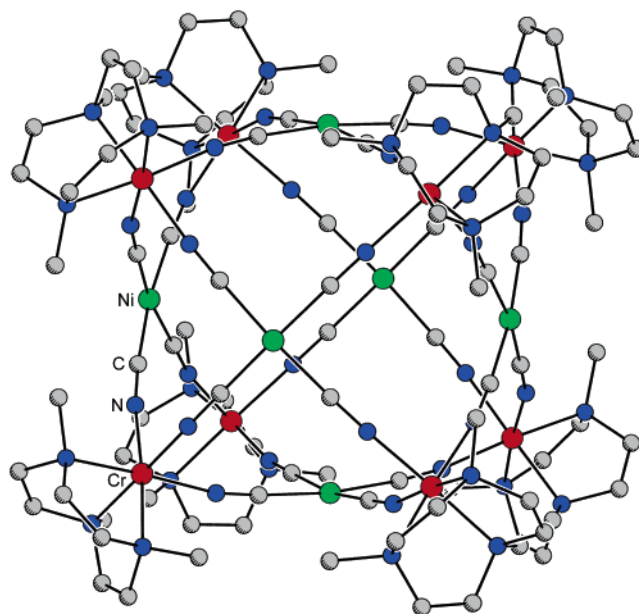


FIGURE 6. Face-centered cubic cluster $[(\text{Me}_3\text{tacn})_8\text{Cr}_8\text{Ni}_6(\text{CN})_{24}]^{12+}$.

In an effort to forestall reorientation of the cyanide ligands and preserve the high-spin character of the Ni^{II} centers, reaction 4 was carried at -40°C in methanol.⁸ Precipitation of the product from solution, again at -40°C , yielded a green solid, which upon warming to room temperature gradually turned orange. This color change can be attributed to isomerization of the cyanide ligands, which, as monitored by infrared spectroscopy, takes 3 days to complete at room temperature. After 3 days, the resulting orange solid is identical in nature to the orange product obtained by carrying out reaction 4 in boiling aqueous solution. Although it has not yet proven possible to crystallize the metastable green form of the compound, we hypothesize that it contains the face-centered cubic cluster $[(\text{Me}_3\text{tacn})_8(\text{H}_2\text{O})_{12}\text{Ni}_6\text{Cr}_8(\text{CN})_{12}]^{12+}$, wherein the carbon ends of the cyanide ligands are still bound to the Cr^{III} centers, and the Ni^{II} centers retain an octahedral coordination geometry by virtue of two axial water ligands. The magnetic properties of the green solid are consistent with this hypothesis. With decreasing temperature, the value of $\chi_{\text{M}}T$ climbs monotonically, indicative of the ferromagnetic coupling expected between Cr^{III} ($S = 3/2$) and high-spin Ni^{II} ($S = 1$). At very low temperature, $\chi_{\text{M}}T$ reaches a value approaching that predicted for an $S = 18$ ground state, as should be attained if all spin centers are in alignment ($8 \times 3/2 + 6 \times 1 = 18$). In addition, at high magnetic field and low temperature, the magnetization of the compound saturates near 36 unpaired electrons, again consistent with an $S = 18$ ground state.

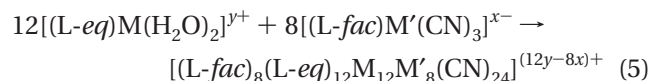
Thus, with metal–cyanide chemistry it is easily possible to generate molecules having exceptionally high spin ground states. In fact, more recent work has uncovered two related cyano-bridged clusters, $(\text{EtOH})_{24}\text{Mn}_9\text{W}_6(\text{CN})_{48}$ and $(\text{MeOH})_{24}\text{Mn}_9\text{Mo}_6(\text{CN})_{48}$, reported as having ground states of $S = 39/2$ and $51/2$, respectively.^{6b,c} The latter value represents a record, which was only recently matched for metal-oxo clusters with the isolation of $[\text{Mn}_{25}\text{O}_{18}(\text{OH})_2(\text{N}_3)_{12}(\text{pdm})_6(\text{pdmH})_6]^{2+}$ ($\text{pdmH}_2 = \text{pyridine-2,6-dimetha-$

nol).¹² Despite their very large S values, none of these molecules possess sufficient magnetic anisotropy to create a spin-reversal barrier greater than that of $[\text{Mn}_{12}\text{O}_{12}(\text{O}_2\text{-CCH}_3)_{16}(\text{H}_2\text{O})_4]$.

As for the cubic $\text{M}_4\text{M}'_4(\text{CN})_{12}$ clusters, substitution of a variety of metal centers into the face-centered cubic geometry is possible. To date, clusters of this type have been structurally characterized with Cr^{III} , low-spin Co^{III} , and Mo^{III} at the corner sites and with low-spin Ni^{II} , Cu^{II} , Pd^{II} , and Pt^{II} at the face-centering sites.^{8,11,13} Aside from the metastable $S = 18$ species incorporating Cr^{III} and high-spin Ni^{II} , no such clusters have yet been reported with paramagnetic metal centers on both sites. Efforts to accomplish this, however, are still underway.

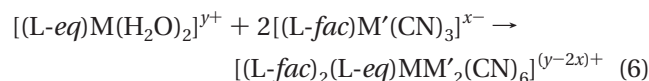
Edge-Bridged Cubic Clusters?

Higher-nuclearity species capable of sustaining even larger spin ground states may also be possible using simple two-component assembly reactions. By combining a trans-directing complex of the type $[(\text{L-}eq)\text{M}(\text{H}_2\text{O})_2]^{y+}$ with an $[(\text{L-fac})\text{M}'(\text{CN})_3]^{x-}$ corner unit in a 12:8 molar ratio, one can potentially generate an edge-bridged cubic cluster containing 20 metal centers:



Here, *L-*eq** is a tetradentate ligand binding four equatorial sites of an octahedrally coordinated metal center M , and the target structure consists of a cube of eight metal centers M' connected along the twelve edges via linear $\text{M}'\text{-CN-M-NC-M}'$ moieties. Alternatively, edge-bridged cubic clusters could be produced through analogous reactions between $[(\text{L-fac})\text{M}(\text{H}_2\text{O})_3]^{x+}$ and $[(\text{L-}eq)\text{M}'(\text{CN})_2]^{y+}$ complexes. The maximum ground-state spin that can be anticipated for this geometry is $S = 26$, as expected with either an antiferromagnetically coupled $\text{Mn}^{\text{II}}_{12}\text{Fe}^{\text{III}}_8(\text{CN})_{24}$ cluster or a ferromagnetically coupled $\text{Ni}^{\text{II}}_8\text{Cr}^{\text{III}}_{12}(\text{CN})_{24}$ cluster. Despite numerous attempts at reaction 5 employing *L-*eq** = *cyclam* = 1,4,8,11-tetraazacyclotetradecane and *L-fac* = *Me₃tacn* or *tach*, an edge-bridged cubic cluster has not yet been obtained—at least not in the form of high-quality single crystals. In some instances, an isomeric two-dimensional honeycomb framework of formula $[(\text{tach})_2(\text{cyclam})_3\text{M}_3\text{Cr}_2(\text{CN})_6]^{6+}$ ($\text{M} = \text{Ni}, \text{Cu}$) instead resulted,¹¹ and in several other attempts, one-dimensional chains retaining one terminal cyanide per M' center crystallized.^{8,11,13}

While the edge-bridged cubic geometry remains elusive, it is often possible to produce a linear edge fragment of the cluster cleanly by employing a 1:2 molar ratio of reactants:



For example, the reaction of $[(\text{cyclam})\text{Ni}(\text{H}_2\text{O})_2]^{2+}$ with two equivalents of $[(\text{Me}_3\text{tacn})\text{Cr}(\text{CN})_3]$ in aqueous solution

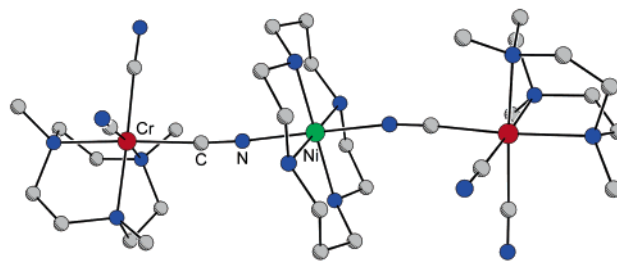


FIGURE 7. Linear cluster $[(\text{Me}_3\text{tacn})_2(\text{cyclam})\text{NiCr}_2(\text{CN})_6]^{2+}$.⁸

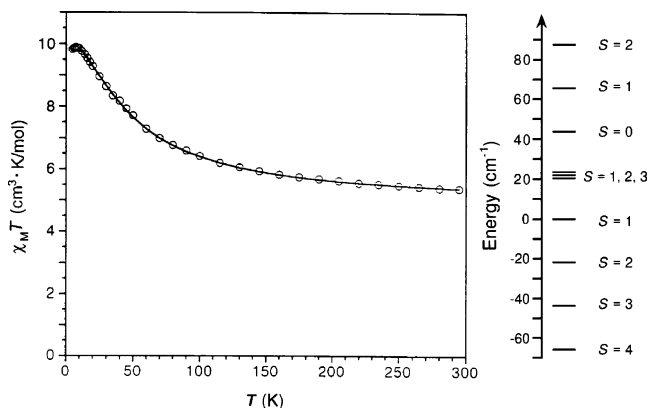


FIGURE 8. Temperature-dependent magnetic behavior (left) of $[(\text{Me}_3\text{tacn})_2(\text{cyclam})\text{NiCr}_2(\text{CN})_6](\text{ClO}_4)_2 \cdot 2\text{H}_2\text{O}$ in an applied field of 1 T.⁸ The solid line represents a calculated fit to the data. On the right, the ground and excited spin-state energies for the linear $\text{Ni}^{\text{II}}\text{Cr}^{\text{III}}_2(\text{CN})_6$ cluster, according to the fit to the data, are shown.

yields the linear species $[(\text{Me}_3\text{tacn})_2(\text{cyclam})\text{NiCr}_2(\text{CN})_6]^{2+}$.⁸ Figure 7 shows the structure of this product, crystallized as its perchlorate salt. Note that it indeed corresponds to a portion of an edge-bridged cubic cluster but with a twist of approximately 124° around the $\text{Cr}^{\text{III}}\text{-CN-Ni}^{\text{II}}\text{-NC-Cr}^{\text{III}}$ axis. Different twist angles are encountered, depending upon the choice of counteranion. The magnetic properties of this trinuclear cluster were studied in detail, since it represents a simple model for the type of exchange that can be expected between Cr^{III} and Ni^{II} in larger cyano-bridged clusters. A plot of the temperature dependence of $\chi_{\text{M}}T$, which is related to the effective magnetic moment through the expression $\mu_{\text{eff}} = 2.828\sqrt{\chi_{\text{M}}T}$, is depicted in Figure 8. At room temperature, $\chi_{\text{M}}T$ is already slightly above the value of $4.75 \text{ cm}^3 \cdot \text{K/mol}$ expected for two Cr^{III} ($S = 3/2$) centers and one high-spin Ni^{II} ($S = 1$) center in the absence of magnetic coupling. The steady rise in $\chi_{\text{M}}T$ with decreasing temperature is indicative of the anticipated ferromagnetic coupling, and the maximum value attained at low temperature is close to the $10.0 \text{ cm}^3 \cdot \text{K/mol}$ expected for the ensuing $S = 4$ ground state. The data were fit with MAGFIT 3.1¹⁴ by employing the following exchange Hamiltonian:

$$\hat{H} = -2J[\hat{S}_{\text{Ni}} \cdot (\hat{S}_{\text{Cr}(1)} + \hat{S}_{\text{Cr}(2)})] \quad (7)$$

This Hamiltonian, together with the ferromagnetic coupling (corresponding to a positive value for J), dictates the ordering of the spin states, as shown at the right in Figure 8. The best fit obtained affords $J = 10.9 \text{ cm}^{-1}$ and $g = 2.00$, where the magnitude of J gives the energy spacing

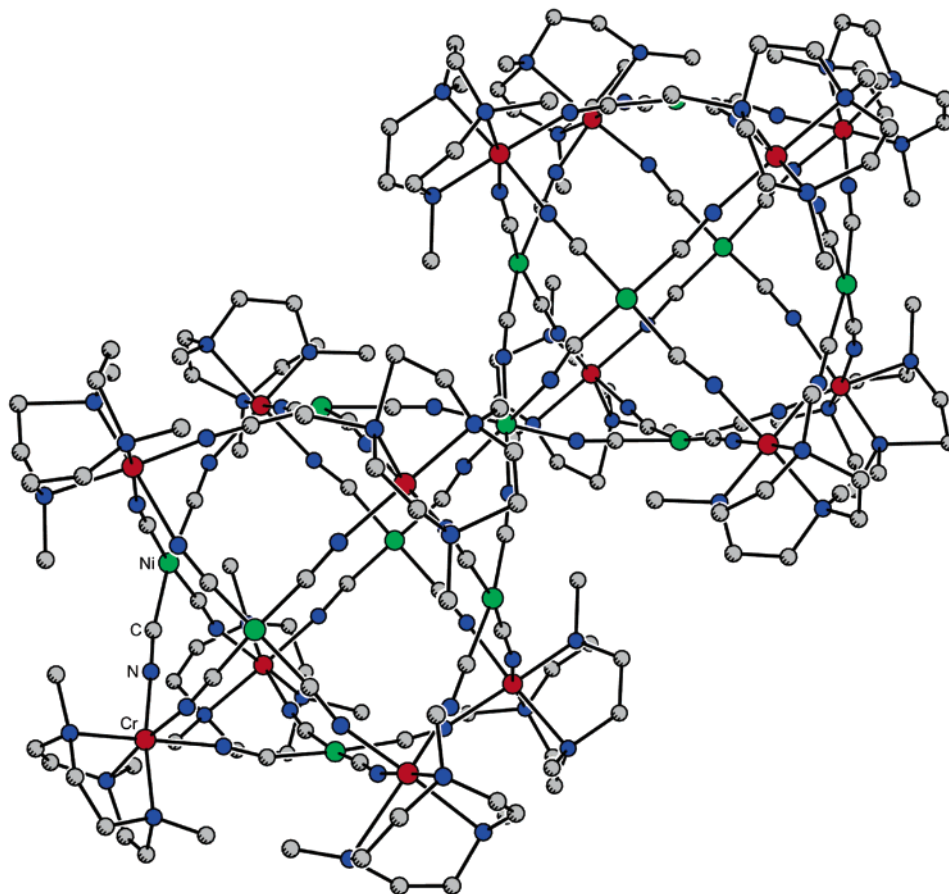


FIGURE 9. Double face-centered cubic cluster $[(\text{Me}_3\text{tacn})_{14}\text{Cr}_{14}\text{Ni}_{13}(\text{CN})_{48}]^{20+}$.¹⁶

between spin states, placing the $S = 4$ ground state just 21.8 cm^{-1} below an $S = 3$ excited state. Magnetization data are consistent with this result and do not indicate any appreciable zero-field splitting in the ground state. Thus, we can expect weak ferromagnetic coupling of approximately this magnitude in larger chromium(III)–nickel(II)–cyanide clusters.

Unexpected Cluster Geometries

Although some degree of control is possible, many assembly reactions do not go according to plan, sometimes giving rise to new, unforeseen cluster geometries. For example, reaction 4 can be successfully executed with use of nickel(II) chloride, bromide, nitrate, or perchlorate, but if nickel(II) iodide is employed, a different product is obtained. In this case, the resulting $\{[(\text{Me}_3\text{tacn})_8\text{Cr}_8\text{Ni}_5(\text{CN})_{24}] \supset \text{I}\}^{9+}$ cluster consists of an incompletely formed face-centered cubic structure, wherein one of the Ni^{II} centers is missing and an iodide anion is situated within the cavity.¹⁵ With four terminal cyanide ligands, this species was found to react with $[\text{Ni}(\text{CN})_4]^{2-}$ in aqueous solution, undergoing a complete rearrangement to form a barrel-shaped cluster of formula $[(\text{Me}_3\text{tacn})_{10}\text{Cr}_{10}\text{Ni}_9(\text{CN})_{42}]^{6+}$.¹⁵ Interestingly, this molecule incorporates all three of the commonly known cyanonickelate complexes: square planar $[\text{Ni}(\text{CN})_4]^{2-}$, square pyramidal $[\text{Ni}(\text{CN})_5]^{3-}$, and trigonal bipyramidal $[\text{Ni}(\text{CN})_5]^{3-}$. Efforts

to produce it directly through stoichiometric assembly reactions, however, instead resulted in isolation of two even larger clusters. The first, obtained from a concentrated solution, is a 24-metal cluster, $[(\text{Me}_3\text{tacn})_{12}\text{Cr}_{12}\text{Ni}_{12}(\text{CN})_{48}]^{12+}$, displaying the edge-bridged cubic structure discussed above but with an additional four Cr^{III} centers capping four of the cube faces.¹⁶ The second, obtained from a more dilute solution, is the 27-metal cluster $[(\text{Me}_3\text{tacn})_{14}\text{Cr}_{14}\text{Ni}_{13}(\text{CN})_{48}]^{20+}$ depicted in Figure 9.¹⁶ Representing the largest metal–cyanide cluster known to date, this species consists of two face-centered cubic units fused though a common corner. Unfortunately, all of these high-nuclearity products result from reactions in which cyanide linkage isomerization affords primarily low-spin Ni^{II} centers. If, however, the putative high-spin precursor to the $\text{Cr}_{14}\text{Ni}_{13}(\text{CN})_{48}$ species can be isolated at low temperature, it should possess an unprecedented $S = 32$ ground state.

With its isotropic electron distribution, assembly reactions involving the Mn^{2+} ion can be particularly difficult to predict. Thus, for example, the reaction between $[\text{Mn}(\text{H}_2\text{O})_6]^{2+}$ and $[(\text{Me}_3\text{tacn})\text{Cr}(\text{CN})_3]$ in aqueous solution does not appear to produce a face-centered cubic cluster. Addition of KClO_4 to the solution, however, permits isolation of $\text{K}[(\text{Me}_3\text{tacn})_6\text{MnCr}_6(\text{CN})_{18}](\text{ClO}_4)_3$, a compound featuring the trigonal prismatic cluster displayed in Figure 10.¹⁷ Here, a single Mn^{II} center is connected to six $[(\text{Me}_3\text{tacn})\text{Cr}(\text{CN})_3]$ complexes through cyanide bridges exhibit-

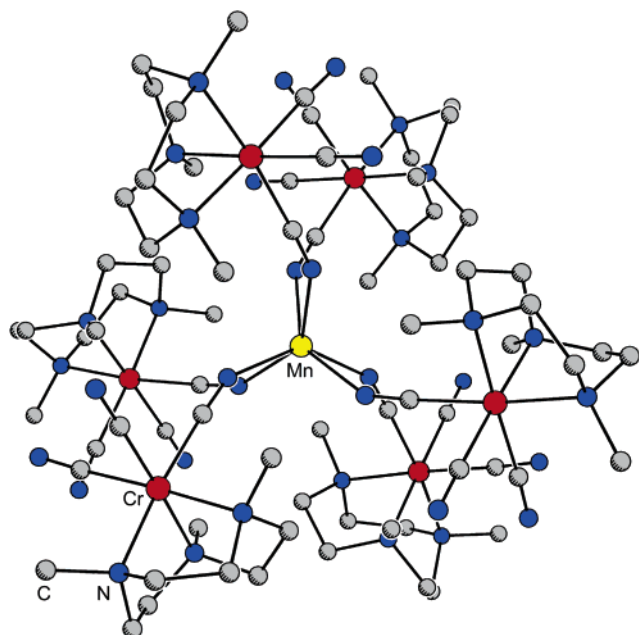


FIGURE 10. Trigonal prismatic cluster $[(\text{Me}_3\text{tacn})_6\text{MnCr}_6(\text{CN})_{18}]^{2+}$.¹⁷

ing significantly bent Mn–N–C angles of $152.7(2)^\circ$. As is typical, the high-spin Mn^{II} ($S = 5/2$) center engages in only weak magnetic exchange interactions with the six surrounding Cr^{III} ($S = 3/2$) centers. Employing the following exchange Hamiltonian, a fit to the variable-temperature magnetic susceptibility data indicates a coupling constant of just $J = -3.1 \text{ cm}^{-1}$.

$$\hat{H} = -2J[\hat{S}_{\text{Mn}} \cdot (\hat{S}_{\text{Cr}(1)} + \hat{S}_{\text{Cr}(2)} + \hat{S}_{\text{Cr}(3)} + \hat{S}_{\text{Cr}(4)} + \hat{S}_{\text{Cr}(5)} + \hat{S}_{\text{Cr}(6)})] \quad (8)$$

Accordingly, the antiferromagnetically coupled cluster possesses an $S = 13/2$ ground state that is not well-isolated in energy. As might be anticipated from the nature of its constituent ions, variable-field magnetization experiments do not reveal any significant zero-field splitting. Although initially formed unexpectedly, as we shall see, it is still possible to substitute different metal ions into this trigonal prismatic geometry.

Instilling Magnetic Anisotropy

Clearly metal–cyanide chemistry can provide access to clusters with high-spin ground states. This, however, is arguably the easier challenge in the quest for new single-molecule magnets; more difficult is how to impart the axial anisotropy requisite in creating a spin-reversal barrier. In particular, we need to develop within the ground state a *negative* axial zero-field splitting, D , in order that the highest magnitude M_S levels are lowest in energy, as diagrammed for an $S = 10$ state in Figure 2. If D is positive, then $M_S = 0$ will be lowest in energy, and there will be no energy cost for losing direction of the spin (i.e., in going from $M_S = +10$ to $M_S = 0$). While we currently have no good means of predicting the sign of D in a complex cluster, we do know that the incorporation of metal ions having a large single-ion anisotropy is necessary for the

overall D to be large in magnitude. The anisotropy of an individual metal ion is associated with coupling between its spin angular momentum and its orbital angular momentum. Consequently, ions with orbitally degenerate ground states will generally have a large zero-field splitting and would be appropriate for incorporation into single-molecule magnets. In $[\text{Mn}_{12}\text{O}_{12}(\text{O}_2\text{CCH}_3)_{16}(\text{H}_2\text{O})_4]$, for example, it is primarily the outer Mn^{III} ions, with a $t_{2g}^3e_g^1$ electron configuration, that contribute to the anisotropy barrier. Hence, an obvious strategy for instilling magnetic anisotropy in metal–cyanide clusters is to utilize metal ions already established as leading to single-molecule magnets in oxo-bridged clusters, specifically, V^{III} , high-spin Mn^{III} , high-spin Fe^{III} , Ni^{II} , and high-spin Co^{II} .^{1,2} Of course, while oxygen-based donor ligands dictate high-spin electron configurations, low-spin configurations will often occur in metal–cyanide clusters, and we should recognize that certain of these with orbital degeneracy may be equally effective.

Our approach will therefore be to attempt to substitute ions with a large individual anisotropy into some of the metal–cyanide cluster geometries already discovered. Note that many of the high-nuclearity clusters produced in simple two-component reactions, such as reactions 3–5 above, approximate O_h symmetry. While such high symmetry does not necessarily preclude development of an overall magnetic anisotropy, it certainly might act against it. Thus, the best candidates for creating single-molecule magnets may be some of the lower symmetry structures, such as those depicted in Figures 7, 9, and 10. This highlights the importance of developing more complex multicomponent or multistep assembly schemes, whereby anisotropic cluster geometries could be more reliably achieved.

Unfortunately, the coordination chemistry of metal ions with orbital angular momentum is often less predictable, making synthesis of the desired precursor complexes more difficult. It is for this reason that the basic exploration of new cluster geometries was not carried out using such ions in the first place. A good example of the type of unexpected reactivity that can be encountered occurred in the course of our attempts to synthesize $[(\text{Me}_3\text{tacn})\text{V}(\text{CN})_3]$ through the reaction of $[(\text{Me}_3\text{tacn})\text{V}(\text{CF}_3\text{SO}_3)_3]$ with LiCN . While two cyanide ligands readily bind the V^{III} center, efforts to attach a third were unsuccessful, leading instead to oligomerization of cyanide to form the tetracyanide-bridged complex $[(\text{Me}_3\text{tacn})_2\text{V}_2(\text{CN})_4(\mu\text{-C}_4\text{N}_4)]$.¹⁸ The structure of this unusual product is displayed in Figure 11 and consists of two V^{IV} ($S = 1/2$) centers, each with a Me_3tacn ligand and two terminal cyanide groups, linked via imido-type coordination at opposing ends of an unprecedented $\text{C}_4\text{N}_4^{4-}$ unit. Magnetic susceptibility data indicate strong antiferromagnetic exchange coupling with $J = -112 \text{ cm}^{-1}$, affording a well-isolated $S = 0$ ground state. Interestingly, reduction of this molecule by one electron produces a class III mixed-valent complex in which the extra electron is delocalized between the two metal centers. The delocalized electron forces the spins at both metal sites into alignment, generating a high-spin

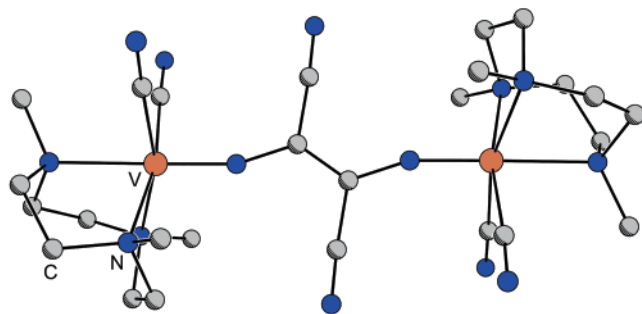


FIGURE 11. Tetracyanide-bridged complex $[(\text{Me}_3\text{tacn})_2\text{V}_2(\text{CN})_4(\mu\text{-C}_4\text{N}_4)]$.¹⁸

$S = 3/2$ ground state through a double-exchange mechanism. Significantly, no population of lower-spin excited states is evident, even at room temperature. The result suggests a means by which mixed-valency might be used in higher-nuclearity species to create high-spin ground states that are very well-isolated in energy.

Another idea for instilling magnetic anisotropy in cyano-bridged clusters is simply to move down the column in the periodic table and utilize second- and third-row transition metal ions. Since spin–orbit coupling is a relativistic phenomenon, this will generally lead to a significant increase in single-ion anisotropy. By replacing the Cr^{III} centers in established metal–cyanide clusters with Mo^{III} centers, we might therefore expect to enhance magnetic anisotropy while preserving the spin of the ground state. Here again, the chemistry is not necessarily so easy. Molybdenum(III) has a larger radius than chromium(III), and indeed reaction of $[(\text{Me}_3\text{tacn})\text{Mo}(\text{CF}_3\text{SO}_3)_3]$ with an excess of LiCN in DMF affords the seven-coordinate complex $[(\text{Me}_3\text{tacn})\text{Mo}(\text{CN})_4]^-$.¹³ Limiting the amount of LiCN employed in the reaction, however, maintains six-coordination with too little producing the cyano-bridged species $[(\text{Me}_3\text{tacn})_2\text{Mo}_2(\text{CN})_5]^+$ and with precisely 3 equiv ultimately permitting isolation of $[(\text{Me}_3\text{tacn})\text{Mo}(\text{CN})_3]$.¹³ Interestingly, a related strategy enabled synthesis of cyano-bridged $[\text{Mo}_2(\text{CN})_{11}]^{5-}$ and the homoleptic octahedral complex $[\text{Mo}(\text{CN})_6]^{3-}$.¹⁹ The former molecule exhibits the strongest magnetic exchange coupling yet observed through a cyanide bridge, with $J = -113 \text{ cm}^{-1}$.

In direct parallel with $[(\text{Me}_3\text{tacn})\text{Cr}(\text{CN})_3]$, 2 equiv of $[(\text{Me}_3\text{tacn})\text{Mo}(\text{CN})_3]$ reacts with $[(\text{cyclam})\text{Ni}(\text{H}_2\text{O})_2]^{2+}$ to produce the linear cluster $[(\text{Me}_3\text{tacn})_2(\text{cyclam})\text{NiMo}_2(\text{CN})_6]^{2+}$.¹³ This molecule adopts the same structure type as the $\text{NiCr}_2(\text{CN})_6$ cluster shown in Figure 7 but with Mo^{III} centers replacing the two Cr^{III} centers. The substitution brings about two significant advantages. First, the valence d orbitals of the second-row transition metal ion are more diffuse, giving rise to better overlap with the cyanide-based orbitals and stronger magnetic exchange coupling. The observed coupling constant J has increased by more than 50% to a value in the range $17.0\text{--}17.6 \text{ cm}^{-1}$, depending slightly on what twist conformation the molecule crystallizes in. Note that the coupling is still ferromagnetic in nature since the t_{2g}^3 electron configuration is retained and, consequently, the molecule still has an $S = 4$ ground state.

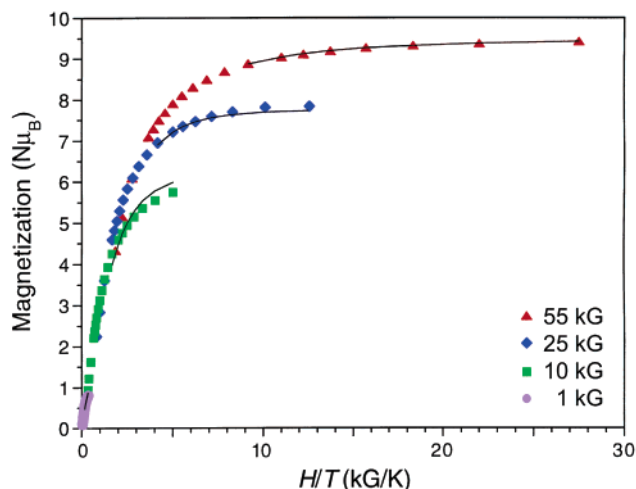


FIGURE 12. Low-temperature magnetization data for $\text{K}[(\text{Me}_3\text{tacn})_6\text{MnMo}_6(\text{CN})_{18}](\text{ClO}_4)_3$.²⁰ Lines represent fits to the data calculated using ANISOFIT.

The second advantage associated with incorporation of Mo^{III} is delivery of the all-important magnetic anisotropy. Variable-field magnetization measurements reveal the presence of substantial zero-field splitting with the best fit to the data for one compound indicating $D = -0.72 \text{ cm}^{-1}$. The sign and magnitude of this D value are supported by high-field, high-frequency electron paramagnetic resonance (EPR) experiments. Thus, with an inferred spin-reversal barrier of $U = S^2|D| = 12 \text{ cm}^{-1}$, $[(\text{Me}_3\text{tacn})_2(\text{cyclam})\text{NiMo}_2(\text{CN})_6]^{2+}$ likely represents the first example of a cyano-bridged single-molecule magnet.

To increase the spin-reversal barrier, we should like to perform similar substitutions in clusters with higher-spin ground states. Accordingly, efforts were made to produce the molybdenum-substituted analogue of the $S = 13/2$ trigonal prismatic cluster $[(\text{Me}_3\text{tacn})_6\text{MnCr}_6(\text{CN})_{18}]^{2+}$ (see Figure 10). Employing a related preparative procedure, use of $[(\text{Me}_3\text{tacn})\text{Mo}(\text{CN})_3]$ indeed led to isolation of $\text{K}[(\text{Me}_3\text{tacn})_6\text{MnMo}_6(\text{CN})_{18}](\text{ClO}_4)_3$.²⁰ This compound is isostructural with its chromium-containing counterpart, containing identical trigonal prismatic cluster units, but with Mo^{III} on the outer six metal sites in place of Cr^{III} . Once again, the substitution has enhanced magnetic exchange coupling, this time more than doubling J to a value of -6.7 cm^{-1} . Variable-temperature magnetization data collected at four selected fields are shown in Figure 12 and nicely demonstrate the effects of zero-field splitting. The isofield lines deviate significantly at low temperature from the simple Brillouin function expected for the spin-only paramagnetism of an $S = 13/2$ ground state. The program ANISOFIT was developed for extracting the zero-field splitting parameters from such data,¹³ in this case affording $D = -0.33 \text{ cm}^{-1}$ and $|E| = 0.018 \text{ cm}^{-1}$.²¹ Thus, the $[(\text{Me}_3\text{tacn})_6\text{MnMo}_6(\text{CN})_{18}]^{2+}$ cluster should behave as a single-molecule magnet with a spin-reversal barrier of $U = 14 \text{ cm}^{-1}$. Note that, despite the increased S value, U is only slightly higher than that for the linear $\text{NiMo}_2(\text{CN})_6$ cluster, owing to a lower overall anisotropy. Very likely, this reduced anisotropy is a result of partial cancellation due to the nonparallel relative orientations of the indi-

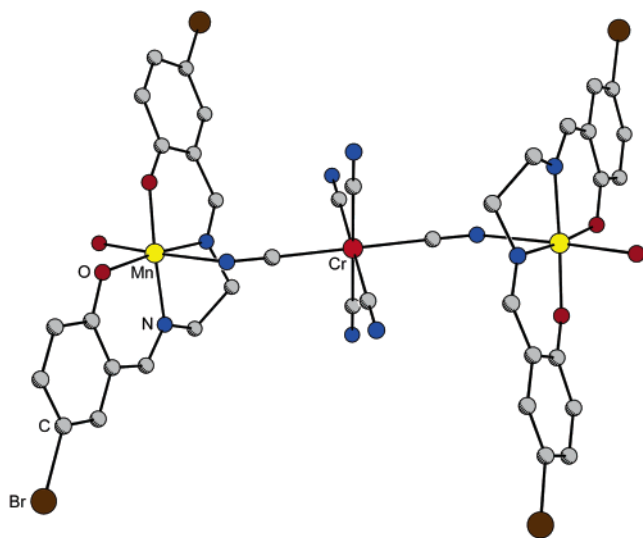
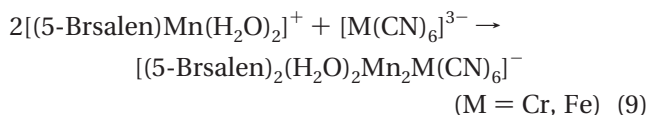


FIGURE 13. Linear cluster $[(5\text{-Brsalen})_2(\text{H}_2\text{O})_2\text{Mn}_2\text{Cr}(\text{CN})_6]^{3-}$.²³

vidual anisotropy axes of the constituent $[(\text{Me}_3\text{tacn})\text{Mo}(\text{CN})_3]$ complexes. Regardless, frequency-dependent AC susceptibility measurements confirm that the compound exhibits slow relaxation of the magnetization with an effective barrier of $U_{\text{eff}} = 10 \text{ cm}^{-1}$.

Ideally, one would like to maximize the anisotropy in a cluster by enforcing a parallel alignment of all of its individual component-ion anisotropy axes. Indeed, this is the situation in $[\text{Mn}_{12}\text{O}_{12}(\text{O}_2\text{CCH}_3)_{16}(\text{H}_2\text{O})_4]$, where the eight outer Mn^{III} centers all have their Jahn–Teller elongation axes aligned roughly perpendicular to the disk of the molecule.¹ The utility of this idea has been demonstrated recently in metal–cyanide clusters through the use of $[(5\text{-Brsalen})\text{Mn}(\text{H}_2\text{O})_2]^+$ (5-Brsalen = *N,N'*-ethylenebis(5-bromosalicylideneiminato)) precursor complexes. Such complexes are well-known to have a Jahn–Teller elongation axis oriented perpendicular to the equatorial coordination plane of the salen ligand. The steric bulk associated with the bromine substituents on the ligand is such that reaction of $[(5\text{-Brsalen})\text{Mn}(\text{H}_2\text{O})_2]^+$ with a hexacyano-metalate complex results in just a trinuclear cluster:^{22,23}



The two products are isostructural, both adopting the linear geometry displayed in Figure 13, wherein two $[(5\text{-Brsalen})\text{Mn}(\text{H}_2\text{O})_2]^+$ moieties are attached to trans nitrogen atoms of the central $[\text{M}(\text{CN})_6]^{3-}$ unit. Although the Jahn–Teller elongation axes of the Mn^{III} centers are not perfectly collinear, they are rigorously parallel. With M = Cr^{III} , the cluster exhibits antiferromagnetic coupling to give an $S = 5/2$ ground state, while with M = Fe^{III} , it exhibits weak ferromagnetic coupling to give an $S = 9/2$ ground state.²³ In both cases, variable-field magnetization data reveal the presence of significant zero-field splitting, and frequency-dependent AC magnetic susceptibility measurements confirm single-molecule-magnet behavior.

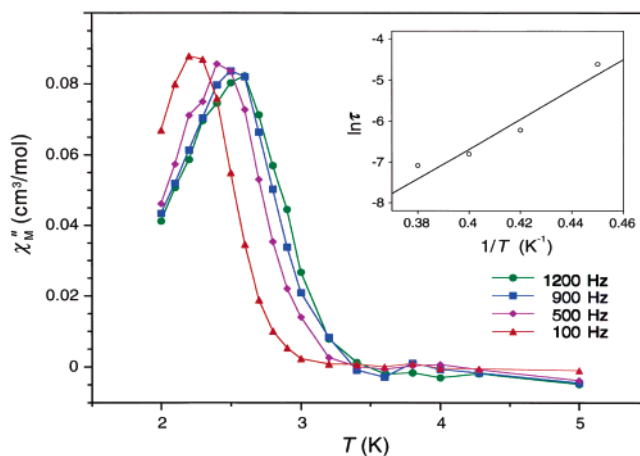


FIGURE 14. Out-of-phase component of the AC susceptibility for $\text{K}[(5\text{-Brsalen})_2(\text{H}_2\text{O})_2\text{Mn}_2\text{Fe}(\text{CN})_6] \cdot 2\text{H}_2\text{O}$.²³ The inset shows the Arrhenius plot of the sample relaxation times with temperature; the solid line is a linear fit to the data, from which U_{eff} is obtained.

These AC susceptibility experiments involve measuring the magnetic susceptibility using a small applied field that switches direction at a fixed frequency. As the frequency is increased to near the relaxation rate, $1/\tau$, for the magnetization of the molecules, a lag is observed in the in-phase susceptibility, χ' . Concomitantly, a rise occurs in the out-of-phase component of the susceptibility, χ'' , which will display a peak with a maximum at the temperature where $1/\tau$ matches the switching frequency. The χ'' data obtained for $\text{K}[(5\text{-Brsalen})_2(\text{H}_2\text{O})_2\text{Mn}_2\text{Fe}(\text{CN})_6] \cdot 2\text{H}_2\text{O}$ are presented in Figure 14. Note how the peaks shift to higher temperatures as the switching frequency increases; this is a classic signature of a single-molecule magnet. Moreover, the Arrhenius relationship between temperature and the magnetization relaxation time, τ , enables determination of the effective spin-reversal barrier, U_{eff} , for the molecules:

$$\ln \tau = \ln \tau_0 + U_{\text{eff}}/(k_{\text{B}}T) \quad (10)$$

Here, the preexponential term τ_0 can be thought of as the relaxation attempt frequency, which can be obtained together with U_{eff} from a linear fit to the data plotted as $\ln \tau$ versus $1/T$ (as shown in the inset of Figure 14). For the linear $\text{Mn}_2\text{Cr}(\text{CN})_6$ and $\text{Mn}_2\text{Fe}(\text{CN})_6$ clusters, such an analysis affords $U_{\text{eff}} = 16$ and 25 cm^{-1} , respectively, with the latter representing the highest spin-reversal barrier yet established for a cyano-bridged single-molecule magnet.

Outlook

While the record spin-reversal barrier of $U_{\text{eff}} = 56 \text{ cm}^{-1}$ in $[\text{Mn}_{12}\text{O}_{12}(\text{O}_2\text{CCH}_2\text{Br})_{16}(\text{H}_2\text{O})_4]$ ³ has not yet been surpassed by a cyano-bridged single-molecule magnet, there are many reasons for optimism. Exploration of the cyanide cluster chemistry of metal ions possessing a large single-ion anisotropy, such as V^{III} , Mn^{III} , and Co^{II} , has only just begun. Even less is known about this type of chemistry for second- and third-row transition metal ions, for which the increased spin–orbit coupling should be of significant advantage. Indeed, obvious improvements to two of the

single-molecule magnets described herein can be anticipated to follow a successful preparation of $[(\text{Me}_3\text{tacn})\text{W}(\text{CN})_3]$. With the added orbital angular momentum, related octahedral building units including metal centers such as Ta^{III} , W^{IV} , Re^{III} , or Re^{V} could be expected to generate even larger anisotropy barriers. Beyond instilling axial anisotropy in a high-spin ground state, it is desirable that the ground state be well-separated in energy from spin-excited states. Here, the choice of bridging ligand is crucial: the stronger the pairwise magnetic exchange coupling, the better isolated the ground state will be. As we have seen, the strength of the exchange through a cyanide bridge is generally somewhat weak, and consequently alternative linear bridging ligands such as 1,4-dicyanamidobenzene and acetylenediide are currently under investigation. For similar reasons, the generation of class III mixed-valent clusters wherein a double-exchange mechanism gives rise to a well-isolated high-spin ground state is being pursued. Clearly, there are ample opportunities for new breakthroughs in the field, and the dream of one day storing information in magnetic molecules provides significant impetus for the research.

We thank the many outstanding co-workers who contributed to this research, whose names appear in the following list of references. We also thank the National Science Foundation, the University of California, Berkeley, the Camille and Henry Dreyfus Foundation, the Alfred P. Sloan Foundation, and Tyco Electronics for funding this research and the Natural Sciences and Engineering Research Council of Canada for partial support of L.M.C.B.

References

- (1) (a) Sessoli, R.; Tsai, H.-L.; Schake, A. R.; Wang, S.; Vincent, J. B.; Folting, K.; Gatteschi, D.; Christou, G.; Hendrickson, D. N. High-Spin Molecules: $[\text{Mn}_{12}\text{O}_{12}(\text{O}_2\text{CR})_{16}(\text{H}_2\text{O})_4]$. *J. Am. Chem. Soc.* **1993**, *115*, 1804–1816. (b) Sessoli, R.; Gatteschi, D.; Caneschi, A.; Novak, M. A. Magnetic Bistability in a Metal-Ion Cluster. *Nature* **1993**, *365*, 141–143.
- (2) Long, J. R. Molecular Cluster Magnets. In *Chemistry of Nanostructured Materials*; Yang, P., Ed.; World Scientific: Hong Kong, 2003; pp 291–315 and references therein.
- (3) Tsai, H.-L.; Chen, D.-M.; Yang, C.-I.; Jwo, T.-Y.; Wur, C.-S.; Lee, G.-H.; Wang, Y. A Single-Molecular Magnet: $[\text{Mn}_{12}\text{O}_{12}(\text{O}_2\text{CCH}_2\text{Br})_{16}(\text{H}_2\text{O})_4]$. *Inorg. Chem. Commun.* **2001**, *4*, 511–514.
- (4) Weihe, H.; Güdel, H. U. Magnetic Exchange Across the Cyanide Bridge. *Comments Inorg. Chem.* **2000**, *22*, 75–103.
- (5) (a) Ferlay, S.; Mallah, T.; Ouahès, R.; Veillet, P.; Verdagner, M. A Room-Temperature Organometallic Magnet Based on Prussian Blue. *Nature* **1995**, *378*, 701–703. (b) Holmes, S. M.; Girolami, G. S. Sol–Gel Synthesis of $\text{KV}^{\text{III}}[\text{Cr}^{\text{III}}(\text{CN})_6]\cdot 2\text{H}_2\text{O}$: A Crystalline Molecule-Based Magnet with a Magnetic Ordering Temperature Above 100 °C. *J. Am. Chem. Soc.* **1999**, *121*, 5593–5594.
- (6) Selected references: (a) Mallah, T.; Auburger, C.; Verdagner, M.; Veillet, P. A Heptanuclear $\text{Cr}^{\text{III}}\text{Ni}^{\text{II}}_6$ Complex with a Low-Lying $S = 15/2$ Ground State. *J. Chem. Soc., Chem. Commun.* **1995**, 61–62. (b) Zhong, Z. J.; Seino, H.; Mizobe, Y.; Hidai, M.; Fujishima, A.; Ohkoshi, S.; Hashimoto, K. A High-Spin Cyanide-Bridged Mn_9W_6 ($S = 39/2$) with a Full-Capped Cubane Structure. *J. Am. Chem. Soc.* **2000**, *122*, 2952–2953. (c) Larionova, J.; Gross, M.; Pilkington, M.; Andres, H.; Stoeckli-Evans, H.; Güdel, H. U.; Decurtins, S. High-Spin Molecules: A Novel Cyano-Bridged $\text{Mn}^{\text{II}}_9\text{Mo}^{\text{V}}_6$ Molecular Cluster with a $S = 51/2$ Ground State and

- Ferromagnetic Intercluster Ordering at Low Temperatures. *Angew. Chem., Int. Ed.* **2000**, *39*, 1605–1609. (d) Berlinguette, C. P.; Vaughn, D.; Cañada-Vilalta, C.; Galán-Mascarós, J. R.; Dunbar, K. R. A Trigonal-Bipyramidal Cyanide Cluster with Single-Molecule-Magnet Behavior: Synthesis, Structure, and Magnetic Properties of $\{[\text{Mn}^{\text{II}}(\text{tmpen})_2]_3[\text{Mn}^{\text{III}}(\text{CN})_6]_2\}$. *Angew. Chem., Int. Ed.* **2003**, *42*, 1523–1526.
- (7) Heinrich, J. L.; Berseth, P. A.; Long, J. R. Molecular Prussian Blue Analogues: Synthesis and Structure of Cubic $\text{Cr}_4\text{Co}_4(\text{CN})_{12}$ and $\text{Co}_8(\text{CN})_{12}$ Clusters. *Chem. Commun.* **1998**, 1231–1232.
 - (8) Berseth, P. A.; Sokol, J. J.; Shores, M. P.; Heinrich, J. L.; Long, J. R. High-Spin Metal-Cyanide Clusters: Assembly of a $\text{Cr}_8\text{Ni}_6(\text{CN})_{24}$ Cage with a Face-Centered Cubic Geometry. *J. Am. Chem. Soc.* **2000**, *122*, 9655–9662.
 - (9) Klausmeyer, K. K.; Rauchfuss, T. B.; Wilson, S. R. Stepwise Assembly of $[(\text{C}_5\text{H}_5)_4(\text{C}_5\text{Me}_5)_4\text{Co}_4\text{Rh}_4(\text{CN})_{12}]^{4+}$, an “Organometallic Box”. *Angew. Chem., Int. Ed.* **1998**, *37*, 1694–1696.
 - (10) Klausmeyer, K. K.; Wilson, S. R.; Rauchfuss, T. B. Alkali Metal-Templated Assembly of Cyanometalate “Boxes” $(\text{NEt}_4)_3[\text{M}(\text{Cp}^*\text{Rh}(\text{CN})_3)_4[\text{Mo}(\text{CO})_3]_4]$, ($\text{M} = \text{K}, \text{Cs}$). Selective Binding of Cs^+ . *J. Am. Chem. Soc.* **1999**, *121*, 2705–2711.
 - (11) Yang, J. Y.; Shores, M. P.; Sokol, J. J.; Long, J. R. High-Nuclearity Metal-Cyanide Clusters: Synthesis, Magnetic Properties, and Inclusion Behavior of Open Cage Species Incorporating $(\text{tacc})\text{M}(\text{CN})_3$ ($\text{M} = \text{Cr}, \text{Fe}, \text{Co}$) Complexes. *Inorg. Chem.* **2003**, *42*, 1403–1419.
 - (12) Murugesu, M.; Habrych, M.; Wernsdorfer, W.; Abboud, K. A.; Christou, G. Single-Molecule Magnets: A Mn_{25} Complex with a Record $S = 51/2$ Spin for a Molecular Species. *J. Am. Chem. Soc.* **2004**, *126*, 4766–4767.
 - (13) Shores, M. P.; Sokol, J. J.; Long, J. R. Nickel(III)-Molybdenum(III)-Cyanide Clusters: Synthesis and Magnetic Behavior of Species Incorporating $[(\text{Me}_3\text{tacn})\text{Mo}(\text{CN})_3]$. *J. Am. Chem. Soc.* **2002**, *124*, 2279–2292.
 - (14) Schmitt, E. A. Ph.D. Thesis, University of Illinois, 1995.
 - (15) Sokol, J. J.; Shores, M. P.; Long, J. R. High-Nuclearity Chromium-Nickel-Cyanide Clusters: An Open $\text{Cr}_8\text{Ni}_{15}(\text{CN})_{24}$ Cage and a C_3 -Symmetric $\text{Cr}_{10}\text{Ni}_9(\text{CN})_{42}$ Cluster Incorporating Three Forms of Cyanonickelate. *Angew. Chem., Int. Ed.* **2001**, *40*, 236–239.
 - (16) Sokol, J. J.; Shores, M. P.; Long, J. R. Giant Metal-Cyanide Coordination Clusters: Tetracapped Edge-Bridged Cubic $\text{Cr}_{12}\text{Ni}_{12}(\text{CN})_{48}$ and Double Face-Centered Cubic $\text{Cr}_{14}\text{Ni}_{13}(\text{CN})_{48}$ Species. *Inorg. Chem.* **2002**, *41*, 3052–3054.
 - (17) Heinrich, J. L.; Sokol, J. J.; Hee, A. G.; Long, J. R. Manganese–Chromium-Cyanide Clusters: Molecular $\text{MnCr}_6(\text{CN})_{18}$ and $\text{Mn}_3\text{Cr}_6(\text{CN})_{18}$ Species and a Related $\text{MnCr}_3(\text{CN})_9$ Chain Compound. *J. Solid State Chem.* **2001**, *159*, 293–301.
 - (18) Shores, M. P.; Long, J. R. Tetracyanide-Bridged Divanadium Complexes: Redox Switching Between Strong Antiferromagnetic and Strong Ferromagnetic Coupling. *J. Am. Chem. Soc.* **2002**, *124*, 3512–3513.
 - (19) Beauvais, L. G.; Long, J. R. Cyanide-Limited Complexation of Molybdenum(III): Synthesis of Octahedral $[\text{Mo}(\text{CN})_6]^{3-}$ and Cyano-Bridged $[\text{Mo}_2(\text{CN})_{11}]^{5-}$. *J. Am. Chem. Soc.* **2002**, *124*, 2110–2111.
 - (20) Sokol, J. J.; Hee, A. G.; Long, J. R. A Cyano-Bridged Single-Molecule Magnet: Slow Magnetic Relaxation in a Trigonal Prismatic $\text{MnMo}_6(\text{CN})_{18}$ Cluster. *J. Am. Chem. Soc.* **2002**, *124*, 7656–7657.
 - (21) Note that it is not always possible to extract the sign of D from magnetization data, and here its assignment as negative is inferred from the observation of slow relaxation of the magnetization.
 - (22) Miyasaka, H.; Matsumoto, N.; Okawa, H.; Re, N.; Gallo, E.; Floriani, C. Complexes Derived from the Reaction of Manganese(III) Schiff Base Complexes and Hexacyanoferrate(III): Syntheses, Multidimensional Network Structures, and Magnetic Properties. *J. Am. Chem. Soc.* **1996**, *118*, 981–994.
 - (23) Choi, H. J.; Sokol, J. J.; Long, J. R. Raising the Spin-Reversal Barrier in Cyano-Bridged Single-Molecule Magnets: Linear $\text{Mn}^{\text{II}}_2\text{M}^{\text{III}}(\text{CN})_6$ ($\text{M} = \text{Cr}, \text{Fe}$) Species Incorporating $[(5\text{-Brsalen})\text{Mn}]^+$ Units. *Inorg. Chem.* **2004**, *43*, 1606–1608.

AR040158E